

Thermal spin current and spin accumulation at ferromagnetic insulator/nonmagnetic metal interface

Y.H. Shen, X.S. Wang,* and X.R. Wang†

Physics Department, The Hong Kong University of Science and Technology, Clear Water Bay, Kowloon, Hong Kong and HKUST Shenzhen Research Institute, Shenzhen 518057, China

Spin current injection and spin accumulation near a ferromagnetic insulator (FI)/nonmagnetic metal (NM) bilayer film under a thermal gradient is investigated theoretically. Using the Fermi golden rule and the Boltzmann equations, we find that FI and NM can exchange spins via interfacial electron-magnon scattering because of the imbalance between magnon emission and absorption caused by either non-equilibrium distribution of magnons or non-equilibrium between magnons and electrons. A temperature gradient in FI and/or a temperature difference across the FI/NM interface generates a spin current which carries angular momenta parallel to the magnetization of FI from the hotter side to the colder one. Interestingly, the spin current induced by a temperature gradient in NM is negligibly small due to the nonmagnetic nature of the non-equilibrium electron distributions. The results agree well with all existing experiments.

PACS numbers: 72.15.Jf, 72.25.Mk, 75.30.Ds, 85.75.-d

I. INTRODUCTION

One of the important topics in spintronics is the spin current generation and detection [1]. Compare with the electron spin current, the magnon spin current has the advantage of lower energy consumption and longer coherence time, especially in ferromagnetic insulators (FI) [2]. Furthermore, magnons can be used to manipulate the motion of magnetic domain walls [3, 4]. Recently, interconversion between electron spin current and magnon spin current and various methods for magnon spin current generation in FI were proposed, such as ferromagnetic resonance (FMR) for coherent magnon spin current generation (known as spin pumping) [2, 5–7] and temperature gradient for incoherent magnon spin current generation (known as spin Seebeck effect) [7–12]. The magnon spin current can be detected by a nonmagnetic metal (NM) such as Pt or Pd with strong spin-orbit couplings by which a spin current can be converted into an electric current via inverse spin Hall effect (ISHE) [13, 14]. Since spin carriers in FI and NM are different (magnons in FI and electrons in NM), the spin transport and spin current conversion between electrons and magnons across the FI/NM interface becomes an interesting and important issue for both the experiment interpretation and potential applications.

Different approaches have been used to investigate the spin transport in FI/NM bilayer. The stochastic LLG equation coupled with “spin mixing conductance” concept [7, 15] describes successfully how a spin current is pumped from FI into NM at FMR or under a temperature gradient [16, 17]. However, the microscopic picture of the spin pumping and spin mixing conductance was not given. A quantum mechanical model based on

interfacial $s - d$ coupling between conducting electrons in NM and local magnetic moments in FI was also proposed [18–21] for spin Seebeck effect (SSE). This model was originally designed for the transverse SSE [9, 11, 18]. In order to explain why spin current in NM changes direction in the higher and the lower temperature sides of a sample, coupling of phonons with spins and electrons is necessary [18] if other effect like the anomalous Nernst effect [22] was not considered. It is believed that a temperature gradient perpendicularly applied to the interface (known as *longitudinal* SSE [11, 12]) is a clean configuration [22] for SSE. In this paper, we investigate the spin transport across FI/NM interface due to interfacial electron-magnon interaction under a perpendicular temperature gradient. Phonons do not dominate spin transport in this case, and are neglected. We show that there is neither spin accumulation nor spin current at thermal equilibrium, in consistent with the laws of thermodynamics. Once there is a temperature gradient in the sample or a temperature difference at the interface, spin accumulation occurs and a spin current flows across the interface. Spins parallel to the magnetization of FI flow from the hotter side to the colder one under a temperature gradient in FI or under a temperature difference across the interface. Surprisingly, a temperature gradient in NM cannot efficiently generate a spin current because the spin currents from non-equilibrium spin-up electrons and spin-down electrons cancel each other, resulting in a negligible contribution. Our results are in good agreement with the present experiments.

II. MODEL AND INTERFACIAL ELECTRON-MAGNON SCATTERING

Following the longitudinal SSE experiments [11], we consider a FI/NM bilayer model as shown in Fig. 1(a). An NM layer is in contact with a FI layer, and two thermal reservoirs of temperatures T_L and T_R are attached to

* Corresponding author: justicewxs@ust.hk

† Corresponding author: phxwan@ust.hk

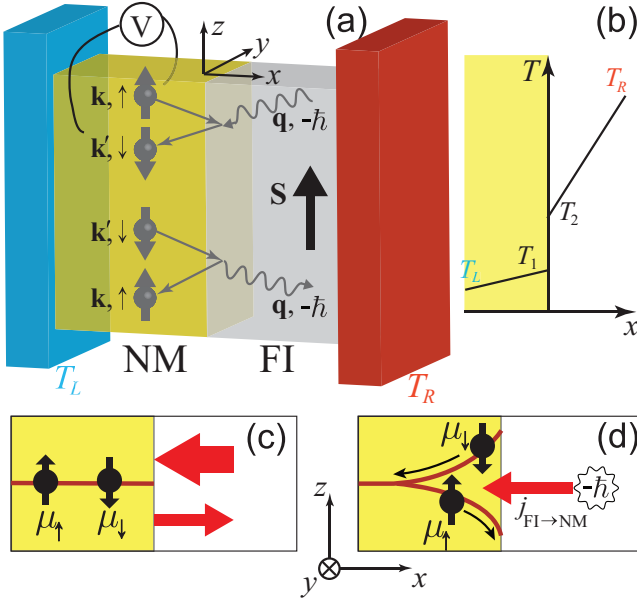


FIG. 1. (color online) (a) The setup of a FI/NM bilayer model and possible electron-magnon scattering process at the interface: a spin-up (spin-down) electron of wavevector \mathbf{k} (\mathbf{k}') becomes a spin-down (spin-up) electron of wavevector \mathbf{k}' (\mathbf{k}) after absorbing (emitting) a magnon of wavevector \mathbf{q} . NM (left) and FI layers (right) are colored yellow and white. The blue and red blocks denote respectively thermal reservoirs of temperature T_L and T_R . (b) Schematic diagram of the temperature profile when $T_R > T_L$. (c) The instant when FI and NM are brought in contact. More magnons flow to the left (thicker arrow) than those to the right (thinner arrow). (d) At the steady state under a thermal gradient, spins flow across the interface and spin accumulation occurs in NM near the FI/NM interface. Spin angular momentum along the $-z$ -direction flows from the hotter side to the colder side.

the left side of NM and the right side of FI. The volume, thickness and lattice constant of FI and NM layers are denoted by V_i , d_i and b_i ($i=\text{FI, NM}$). The interface is in the yz -plane and its area is A . Although most insulators used in SSE experiments are ferrimagnetic, the energy of inter-sublattice excitations is too high to be excited at low temperature [18, 23]. Only the acoustic spin waves are relevant so that FIs are considered. A FI can be modeled by the Heisenberg model of spin S on cubic lattice. The electrons in NM are modeled as a free-electron gas. Without losing generality, magnetization of FI is in the $-z$ -direction so that atomic spins \mathbf{S} are in the $+z$ -direction due to the negative gyromagnetic ratio. The z -component of spins carried by spin-up (spin-down) electrons and magnons are $\frac{\hbar}{2}$ ($-\frac{\hbar}{2}$) and $-\hbar$ respectively in our model. The current density of spins along $-z$ -direction in NM is $\mathbf{j}_s = (\frac{\hbar}{2e})\mathbf{j}_\uparrow - (\frac{\hbar}{2e})\mathbf{j}_\downarrow$, where $\mathbf{j}_{\uparrow(\downarrow)}$ is the electric current density carried by spin-up (spin-down) electrons and $e > 0$ is the absolute value of the electron charge.

The interaction between electrons in NM and local

magnetic moment is modeled by an interfacial $s-d$ Hamiltonian [24, 25],

$$H = -\mathcal{J}_{sd} b_{\text{FI}}^3 \sum_n \mathbf{s} \cdot \mathbf{S}_n \delta(\mathbf{r} - \mathbf{R}_n), \quad (1)$$

where \mathbf{s} is itinerant electron spin in NM and \mathbf{S}_n is local atomic spin at site n of position \mathbf{R}_n on the interface. \mathbf{s} and \mathbf{S}_n are in the units of \hbar . \mathcal{J}_{sd} is the $s-d$ coupling strength and the summation is over the atom sites on the interface. To calculate interfacial electron-magnon scattering rate, we use the lowest-order Holstein-Primakoff transformation [26] $S_{n-} = \sqrt{2S}a_n^\dagger$ and $S_{n+} = \sqrt{2S}a_n$ (S_{n+} and S_{n-} are ladder operators of \mathbf{S}_n at site n and a_n^\dagger , a_n are the corresponding creation and annihilation operators of magnons) so that magnon-magnon interactions are neglected. The scattering due to the non-spin-flipping part of H do not contribute to spin current and spin accumulation, and is neglected. In the momentum space, H involving spin-flipping can be written as,

$$H' = -\mathcal{J}_{sd} \frac{b_{\text{FI}}^3 N_{\text{IN}}}{V_{\text{NM}}} \sqrt{\frac{S}{2N_{\text{FI}}}} \times \sum_{\mathbf{k}, \mathbf{k}', \mathbf{q}} (c_{\mathbf{k}\uparrow}^\dagger c_{\mathbf{k}'\downarrow} a_{\mathbf{q}}^\dagger + c_{\mathbf{k}'\downarrow}^\dagger c_{\mathbf{k}\uparrow} a_{\mathbf{q}}) \delta_{\mathbf{k}'_\parallel - \mathbf{k}_\parallel = \mathbf{q}_\parallel}, \quad (2)$$

where $c_{\mathbf{k}\uparrow}^\dagger$ ($c_{\mathbf{k}\uparrow}$) and $c_{\mathbf{k}\downarrow}^\dagger$ ($c_{\mathbf{k}\downarrow}$) are the creation (annihilation) operators of spin-up and spin-down electrons of wavevector \mathbf{k} , respectively. $a_{\mathbf{q}}^\dagger$ ($a_{\mathbf{q}}$) is the creation (annihilation) operator of magnons of wavevector \mathbf{q} . N_{FI} and N_{IN} are the numbers of atomic spins in FI and at the interface, respectively. The first (second) term describes an incident spin-down (spin-up) electron of wavevector \mathbf{k}' (\mathbf{k}) emitting (absorbing) a magnon of wavevector \mathbf{q} and becoming an outgoing spin-up (spin-down) electron of wavevector \mathbf{k} (\mathbf{k}'), as illustrated in Fig. 1(a). This Hamiltonian preserves angular momentum, and the momentum parallel to the interface is conserved.

Similar to the usual phonon-electron scattering calculation [27] by the Fermi golden rule, the magnon emission and absorption rates between electron states \mathbf{k} and \mathbf{k}' are

$$t_{\text{em}} = S \frac{\pi}{\hbar} \frac{\mathcal{J}_{sd}^2}{V_{\text{NM}}^2} \frac{N_{\text{IN}}^2}{N_{\text{FI}}} [n(\mathbf{q}) + 1] \delta(E_{\mathbf{k}} + \varepsilon_{\mathbf{q}} - E_{\mathbf{k}'}) \delta_{\mathbf{k}'_\parallel - \mathbf{k}_\parallel = \mathbf{q}_\parallel},$$

$$t_{\text{ab}} = S \frac{\pi}{\hbar} \frac{\mathcal{J}_{sd}^2}{V_{\text{NM}}^2} \frac{N_{\text{IN}}^2}{N_{\text{FI}}} n(\mathbf{q}) \delta(E_{\mathbf{k}} + \varepsilon_{\mathbf{q}} - E_{\mathbf{k}'}) \delta_{\mathbf{k}'_\parallel - \mathbf{k}_\parallel = \mathbf{q}_\parallel},$$

where $n(\mathbf{q})$ is the number of magnons of wavevector \mathbf{q} , $E_{\mathbf{k}}$ and $\varepsilon_{\mathbf{q}}$ are electron energy of wavevector \mathbf{k} and magnon energy of wavevector \mathbf{q} , respectively. According to the physical picture illustrated in Fig. 1(a), the perpendicular wavevector components should satisfy $k'_x > 0$, $k_x < 0$, $q_x > 0$ for magnon emission and $k_x > 0$, $k'_x < 0$, $q_x < 0$ for absorption. For simplicity, a quadratic dispersion is assumed for electrons in NM, $E_{\mathbf{k}} = \frac{\hbar^2 |\mathbf{k}|^2}{2m}$. The magnon spectrum is $\varepsilon_{\mathbf{q}} = J|\mathbf{q}|^2 + D$ where J is the ferromagnetic exchange coupling and D is the gap due to magnetic anisotropy.

The net spin current density $j_{\text{FI} \rightarrow \text{NM}}$ at the interface is defined as the angular momentum parallel to the magnetization of FI cross the interface per unit area and per unit time, which is proportional to the difference of the absorbed magnon number N_{ab} and the emitted one N_{em} per unit time,

$$j_{\text{FI} \rightarrow \text{NM}} = \hbar \frac{N_{\text{ab}} - N_{\text{em}}}{A}. \quad (3)$$

By including the Pauli principle for electrons, N_{ab} and N_{em} can be obtained from t_{ab} and t_{em} ,

$$\begin{aligned} N_{\text{em}} &= \sum_{\mathbf{k}, \mathbf{k}', \mathbf{q}} f_{\downarrow}(\mathbf{k}') [1 - f_{\uparrow}(\mathbf{k})] t_{\text{em}}, \\ N_{\text{ab}} &= \sum_{\mathbf{k}, \mathbf{k}', \mathbf{q}} f_{\uparrow}(\mathbf{k}) [1 - f_{\downarrow}(\mathbf{k}')] t_{\text{ab}}, \end{aligned} \quad (4)$$

where $f_s(\mathbf{k})$ is the electron distribution function of wavevector \mathbf{k} and spin $s = \uparrow, \downarrow$. For a macroscopic system the summation can be converted into integration by $\sum_{\mathbf{k}, \mathbf{k}', \mathbf{q}} \delta_{\mathbf{k}' - \mathbf{k} \parallel = \mathbf{q} \parallel} \rightarrow \frac{V_{\text{NM}} V_{\text{NM}}}{(2\pi)^3} \frac{d_{\text{FI}}}{2\pi} \int \delta(\mathbf{k} \parallel + \mathbf{q} \parallel - \mathbf{k}' \parallel) d\mathbf{k} d\mathbf{k}' d\mathbf{q}$. The range of integration is $k_x > 0, k'_x < 0, q_x < 0$ for magnon absorption and $k'_x > 0, k_x < 0, q_x > 0$ for emission. \mathbf{q} is in the first Brillouin Zone. To combine two integrals in Eq. (4) together, we change the dummy variables in N_{em} as $\mathbf{k} \rightarrow -\mathbf{k}, \mathbf{k}' \rightarrow -\mathbf{k}'$ and $\mathbf{q} \rightarrow -\mathbf{q}$. The spin current becomes

$$j_{\text{FI} \rightarrow \text{NM}} = \hbar C \int_{\text{all}} \{ f_{\uparrow}(\mathbf{k}) [1 - f_{\downarrow}(\mathbf{k}')] n(\mathbf{q}) - f_{\downarrow}(-\mathbf{k}') [1 - f_{\uparrow}(-\mathbf{k})] [n(-\mathbf{q}) + 1] \} \quad (5)$$

with $C = \frac{\pi}{\hbar} \frac{S \mathcal{J}_{sd}^2 t_{\text{FI}}^5}{(2\pi)^7}$. Here $\int_{\text{all}} = \int \delta(E_{\mathbf{k}} + \varepsilon_{\mathbf{q}} - E_{\mathbf{k}'}) \delta(\mathbf{k} \parallel + \mathbf{q} \parallel - \mathbf{k}' \parallel) d\mathbf{k} d\mathbf{k}' d\mathbf{q}$ with $k_x > 0, k'_x < 0, q_x < 0$ and $\mathbf{q} \in \text{Brillouin Zone}$.

III. SPIN TRANSPORT AT THERMAL EQUILIBRIUM

First we consider the case of the bilayer at thermal equilibrium ($T_L = T_R = T$). The magnon number follows the Bose-Einstein distribution $n(\mathbf{q}) = n_0(\mathbf{q}) = \frac{1}{e^{\beta \varepsilon_{\mathbf{q}}} - 1}$ and the electron distribution function is the Fermi-Dirac function $f_s(\mathbf{k}) = f_0(\mathbf{k}) = \frac{1}{e^{\beta(E_{\mathbf{k}} - \mu_s)} + 1}$, where $s = \uparrow, \downarrow$, $\beta = (k_B T)^{-1}$ and k_B is the Boltzmann constant. Because electrons are unpolarized in NM, the chemical potentials of spin-up and spin-down electrons must be the same, $\mu_{\uparrow} = \mu_{\downarrow} = \mu_0$, at the instant when FI and NM are brought to contact. Due to the energy conservation $E_{\mathbf{k}} + \varepsilon_{\mathbf{q}} = E_{\mathbf{k}'}$, we have

$$\begin{aligned} & f_0(\mathbf{k}) [1 - f_0(\mathbf{k}')] n_0(\mathbf{q}) \\ &= \frac{1}{e^{\beta(E_{\mathbf{k}} - \mu_0)} + 1} \frac{e^{\beta(E_{\mathbf{k}' - \mu_0)}}}{e^{\beta(E_{\mathbf{k}' - \mu_0)} + 1}} \frac{1}{e^{\beta \varepsilon_{\mathbf{q}}} - 1} \\ &= \frac{1}{e^{\beta(E_{\mathbf{k}} - \mu_0)} + 1} \frac{e^{\beta(E_{\mathbf{k}} - \mu_0)} e^{\beta \varepsilon_{\mathbf{q}}}}{e^{\beta(E_{\mathbf{k}' - \mu_0)} + 1}} \frac{1}{e^{\beta \varepsilon_{\mathbf{q}}} - 1} \\ &= f_0(-\mathbf{k}') [1 - f_0(-\mathbf{k})] [n_0(-\mathbf{q}) + 1]. \end{aligned} \quad (6)$$

Eq. (6) is the detailed balance between magnon absorption and magnon emission at the thermal equilibrium. Using this detailed balance result, Eq. (5) gives a vanishing spin current, $j_{\text{FI} \rightarrow \text{NM}} = 0$, and no spin accumulation in this case. In fact, no spin current and no spin accumulation at the thermal equilibrium hold in general. Otherwise, a spin current would convert into charge current via the ISHE effect. Thus, this device would generate electricity at the thermal equilibrium! Since no external energy source exists in the set-up, this assumption leads to a continuous extraction of electric energy from a sole heat bath, a clear violation of the second law of thermodynamics. Thus, our result must be model independent and true in general. Also, if one regards spin accumulation as a proximity effect of a NM in contact with a FI, this result says that the proximity effect does not exist at the thermal equilibrium, very different from other types of proximity effects such as a semiconductor carbon nanotube in contact with a metallic carbon nanotube [28]. There, the semiconductor carbon nanotube becomes a weak metal at the thermal equilibrium.

IV. SPIN TRANSPORT AT NON-EQUILIBRIUM

When different temperatures T_L, T_R are applied on the two sides of the FI/NM bilayer as shown in Fig. 1(a), the system is at a non-equilibrium state and thermal gradients will eventually established in both FI and NM. Also, a temperature difference across the FI/NM interface may exist when the thermal contact resistance is non-zero. The temperature profile can in principle be obtained by solving the corresponding heat diffusion equations with proper boundary conditions if the thermal conductivities and other material parameters are known. Since the temperature profile is not the subject of this work, we shall simply assume constant thermal conductivities κ_i of the materials ($i = \text{FI}, \text{NM}$), and a constant thermal contact resistance R [11, 29, 30]. Thus, as shown in Fig. 1(b), a uniform temperature gradient of $\alpha_{\text{NM}} = (T_1 - T_L)/d_{\text{NM}}$ in NM, a uniform temperature gradient of $\alpha_{\text{FI}} = (T_R - T_2)/d_{\text{FI}}$ in FI, and an interfacial temperature difference $\Delta T \equiv T_2 - T_1$ across the interface are established at the steady state. $\alpha_{\text{NM}}, \alpha_{\text{FI}}$ and ΔT satisfy

$$\begin{aligned} \alpha_{\text{NM}} d_{\text{NM}} + \Delta T + \alpha_{\text{FI}} d_{\text{FI}} &= T_R - T_L, \\ \alpha_{\text{NM}} \kappa_{\text{NM}} &= \frac{\Delta T}{R} = \alpha_{\text{FI}} \kappa_{\text{FI}}. \end{aligned}$$

α_{NM} will induce a non-equilibrium distribution of electrons, while α_{FI} will induce a non-equilibrium distribution of magnons. ΔT will break the detailed balance between the magnon absorption and emission as shown in section III. Since the magnon emission and absorption are no longer balanced, a net spin current across the interface shall appear.

On the other hand, due to the spin conserved $s-d$ interaction at the interface, each absorbed magnon results in an electron to flip from spin-up to spin-down state, and each emitted magnon causes an electron to flip from spin-down to spin-up state. Thus, if there are more absorbed magnons than emitted ones ($j_{\text{FI} \rightarrow \text{NM}} > 0$ according to Eq. (3)), the number of spin-down electrons would be larger than that of spin-up electrons, and chemical potential of spin-up and spin-down electrons would no longer be the same and $\mu_{\downarrow} > \mu_{\uparrow}$. Similarly, when $j_{\text{FI} \rightarrow \text{NM}} < 0$, we have $\mu_{\uparrow} > \mu_{\downarrow}$. The electron spin accumulation near the interface causes a spin current \mathbf{j}_s in NM due to spin diffusion. This spin current should be continuum at the interface. Thus we have

$$-j_{\text{FI} \rightarrow \text{NM}} = j_s(0) = \left(\frac{\hbar}{2e}\right) j_{\uparrow}(0) + \left(-\frac{\hbar}{2e}\right) j_{\downarrow}(0). \quad (7)$$

Both $j_{\uparrow(\downarrow)}$ and $j_{\text{FI} \rightarrow \text{NM}}$ can be determined by the distribution functions of electrons and magnons, which will be studied by solving the Boltzmann equations in the next subsection.

A. Distribution functions under given temperature profile

When the system is not far from the equilibrium, $n(\mathbf{q})$ and $f_s(\mathbf{k})$ ($s = \uparrow, \downarrow$) are govern by the Boltzmann equations with the relaxation time approximation. For magnons, the distribution function $n(\mathbf{q})$ under the thermal gradient α_{FI} can be obtained by solving following Boltzmann equation

$$\mathbf{v}(\mathbf{q}) \cdot \nabla n(\mathbf{q}) = -\frac{n_1(\mathbf{q})}{\tau}, \quad (8)$$

where $\mathbf{v}(\mathbf{q}) = \frac{1}{\hbar} \nabla_{\mathbf{q}} \varepsilon_{\mathbf{q}}$ is the group velocity of magnons with wavevector \mathbf{q} , τ is the average relaxation time of magnons, and $n_1(\mathbf{q}) = n(\mathbf{q}) - n_0(\mathbf{q})$ where $n_0(\mathbf{q}) = \frac{1}{e^{\beta \varepsilon_{\mathbf{q}}} - 1}$ is the Bose-Einstein distribution with the local temperature. To the first order in α_{FI} , we can replace $n(\mathbf{q})$ by $n_0(\mathbf{q})$ in Eq. (8), and obtain

$$n(\mathbf{q}) = n_0(\mathbf{q}) - \tau v_x(\mathbf{q}) \alpha_{\text{FI}} \frac{\partial n_0(\mathbf{q})}{\partial T}, \quad (9)$$

where $\frac{\partial n_0}{\partial T} = \frac{\beta \varepsilon_{\mathbf{q}}}{T} n_0(n_0 + 1)$. Obviously, we have $n_1(-\mathbf{q}) = -n_1(\mathbf{q})$.

For electrons, the non-equilibrium distribution is not only affected by the temperature gradient α_{NM} , but also by the spin accumulation near the interface, as shown in Fig. 1(d). To take this spin accumulation into consideration, we need to solve the Boltzmann equation about $f_s(\mathbf{k}, \mathbf{r})$ including the spin-flip process [20, 33, 34]:

$$\mathbf{v} \cdot \nabla f_s + \left(-\frac{e\mathcal{E}}{\hbar}\right) \cdot \nabla_{\mathbf{k}} f_s = -\frac{f_s - f_{0,s}}{\tau_c} - \frac{f_{0,s} - f_{0,-s}}{\tau_{sf}}, \quad (10)$$

where $\mathbf{v} = \frac{\hbar \mathbf{k}}{m}$, $f_{0,s} = [e^{\beta(E - \mu_s)} + 1]^{-1}$ is the equilibrium distribution function with local temperature and local electrochemical potential $\mu_s(x)$ for spin s . The relaxation times τ_c and τ_{sf} describe respectively the momentum-energy relaxation and spin relaxation of electrons. $\mathcal{E} = -\nabla \phi$ is the electric field in NM, and $E = \frac{\hbar^2 k^2}{2m} - e\phi$ is the electron energy. To solve Eq. (10) in linear response regime ($f_{1,s}$ linear in the temperature gradient and electric field), we can replace f_s by $f_{0,s}$ in the left-hand side of Eq. (10). Thus, we obtain

$$\begin{aligned} \mathbf{v} \cdot \left[\frac{-\nabla T}{T} (E - \mu_s) - \nabla \mu_s \right] \frac{\partial f_{0,s}}{\partial E} \\ = -\frac{f_s - f_{0,s}}{\tau_c} - \frac{f_{0,s} - f_{0,-s}}{\tau_{sf}}. \end{aligned} \quad (11)$$

Normally, the deviation of the local electrochemical potential $\delta \mu_s = \mu_s - \mu_e$ from the electrochemical potential without spin accumulation (μ_e) is small. Since the change of the density of state near the Fermi surface is small, it is common to use the approximation of $\delta \mu_{\uparrow} = -\delta \mu_{\downarrow}$ [20, 31, 32]. After expanding μ_s and $f_{0,s}$ at μ_e and keeping the linear terms in Eq. (11), we have

$$f_s(\mathbf{k}) = f_0(\mathbf{k}) - \left(1 - 2\frac{\tau_c}{\tau_{sf}}\right) \delta \mu_s \frac{\partial f_0(\mathbf{k})}{\partial E} + g_s(\mathbf{k}), \quad (12)$$

where

$$g_s(\mathbf{k}) = \tau_c v_x(\mathbf{k}) \left[\frac{\alpha_{\text{NM}}}{T} (E_k - \mu_e) + \frac{d\mu_e}{dx} + \frac{d\delta \mu_s}{dx} \right] \frac{\partial f_0(\mathbf{k})}{\partial E},$$

and $f_0 = [e^{\beta(E - \mu_e)} + 1]^{-1}$ is the Fermi-Dirac distribution function without spin accumulation. Because $\tau_c \ll \tau_{sf}$ in most cases, we can discard $2\frac{\tau_c}{\tau_{sf}}$ in Eq. (12). Obviously, we have $g_s(-\mathbf{k}) = -g_s(\mathbf{k})$ and $f_{1,s}(\mathbf{k}) = f_s(\mathbf{k}) - f_0(\mathbf{k}) = -\delta \mu_s \frac{\partial f_0(\mathbf{k})}{\partial E} + g_s(\mathbf{k})$.

Since $\frac{d\mu_e}{dx}$ and $\frac{d\delta \mu_{\uparrow}}{dx} = -\frac{d\delta \mu_{\downarrow}}{dx}$ are still unknown, we need to consider the charge/spin transport in NM. In NM where $(f_{\uparrow} + f_{\downarrow}) = 2f_0 + 2\tau_c v_x \left[\frac{\alpha_{\text{NM}}}{T} (E - \mu_e) + \frac{d\mu_e}{dx} \right] \frac{\partial f_0}{\partial E}$, the electric current

$$j = \frac{(-e)}{V_{\text{NM}}} \sum_{\mathbf{k}} 2\tau_c v_x^2 \left[\frac{\alpha_{\text{NM}}}{T} (E - \mu_e) + \frac{d\mu_e}{dx} \right] \frac{\partial f_0}{\partial E} \quad (13)$$

is not affected by the spin accumulation, and the spin current

$$j_s = -\frac{\hbar}{2V_{\text{NM}}} \sum_{\mathbf{k}} v_x (f_{\uparrow} - f_{\downarrow}) = \frac{\hbar \sigma}{2e^2} \frac{d\delta \mu_{\uparrow}}{dx} \quad (14)$$

depends on the spin accumulation. $\sigma = \frac{ne^2 \tau_c}{m}$ is the conductivity of the metal, n is the electron density in the NM.

The distribution of $\delta \mu_{\uparrow}$ inside NM can be determined by the diffusion equation [20, 31–34]:

$$\frac{d^2 \delta \mu_{\uparrow}}{dx^2} = \frac{\delta \mu_{\uparrow}}{l_{sd}^2},$$

where l_{sd} is the spin diffusion length. For $d_{\text{NM}} \gg l_{sd}$, $\delta\mu_{\uparrow}(x) = \delta\mu_{\uparrow}(0) \exp(x/l_{sd})$, and

$$\frac{d\delta\mu_{\uparrow}}{dx} = \frac{\delta\mu_{\uparrow}}{l_{sd}}. \quad (15)$$

$\frac{d\mu_e}{dx}$ can be determined from the fact that there is no electric current in an open circuit, Eq. (13) gives

$$\frac{d\mu_e}{dx} = -\frac{\alpha_{\text{NM}} \int v^2 (E - \mu_e) \frac{\partial f_0}{\partial E} d^3\mathbf{k}}{T \int v^2 \frac{\partial f_0}{\partial E} d^3\mathbf{k}} \approx -\frac{\alpha_{\text{NM}} (\pi k_{\text{B}} T)^2}{2T \mu_e}. \quad (16)$$

This is the conventional Seebeck effect [35].

To fully determine $f_s(\mathbf{k})$, one still needs to find out $\delta\mu_{\uparrow}(0)$ in terms of known model parameters. The right hand side of Eq. (7) is linear in $\delta\mu_{\uparrow}(0)$ after using expression found early for j_s and $\frac{d\delta\mu_{\uparrow}}{dx} = \frac{\delta\mu_{\uparrow}}{l_{sd}}$. $j_{\text{FI} \rightarrow \text{NM}}$ in Eq. (7) can also be expressed by $n(\mathbf{q})$ and $f_s(\mathbf{k})$ as given by Eq. (5). Thus Eq. (7) would be an equation about $\delta\mu_{\uparrow}(0)$. Then we can obtain the spin accumulation and spin current across the interface as shown below.

B. Spin current in linear response regime

In the last subsection, we obtained $f_s(\mathbf{k}) = f_0(\mathbf{k}) + f_{1,s}(\mathbf{k})$ and $n(\mathbf{q}) = n_0(\mathbf{q}) + n_1(\mathbf{q})$, where $f_{1,s}$ and n_1 , linear in thermal gradient, is much smaller than their equilibrium values. Substitute them into Eq. (5) and keep only the terms up to linear orders in $f_{1,s}$ and n_1 , the spin current can be decomposed into three terms:

$$j_{\text{FI} \rightarrow \text{NM}} = j_d + j_m + j_e, \quad (17)$$

where

$$j_d = \hbar C \int_{\text{all}} \{f_0(\mathbf{k})[1 - f_0(\mathbf{k}')]n_0(\mathbf{q}) - f_0(\mathbf{k}')[1 - f_0(\mathbf{k})][n_0(\mathbf{q}) + 1]\}, \quad (18)$$

$$j_m = \hbar C \int_{\text{all}} \{f_0(\mathbf{k})[1 - f_0(\mathbf{k}')]n_1(\mathbf{q}) - f_0(\mathbf{k}')[1 - f_0(\mathbf{k})]n_1(-\mathbf{q})\}, \quad (19)$$

$$j_e = \hbar C \int_{\text{all}} \{f_{1,\uparrow}(\mathbf{k})[1 - f_0(\mathbf{k}')] - f_0(\mathbf{k})f_{1,\downarrow}(\mathbf{k}')\}n_0(\mathbf{q}) - \{f_{1,\downarrow}(-\mathbf{k}')[1 - f_0(\mathbf{k})] - f_0(\mathbf{k}')f_{1,\uparrow}(-\mathbf{k})\}[n_0(\mathbf{q}) + 1], \quad (20)$$

where $f_0 = \frac{1}{e^{\beta_1(E - \mu_e)} + 1}$ and $n_0 = \frac{1}{e^{\beta_2 \varepsilon} - 1}$ with $\beta_1 = \frac{1}{k_{\text{B}} T_1}$, $\beta_2 = \frac{1}{k_{\text{B}} T_2}$. T_1 and T_2 are the temperatures of NM and FI at the FI/NM interface.

Since Eq. (6) is no longer valid if $\beta_1 \neq \beta_2$, j_d is not zero in this case. j_m is mainly due to the deviation of magnons from their equilibrium distribution. If there is no temperature gradient α_{FI} , Eq. (9) says $n_1 = 0$, and

then j_m vanishes. j_e comes from the deviation of electrons from their equilibrium distribution. According to Eq. (12), the deviation is caused by both temperature gradient α_{NM} as well as the spin accumulation $\delta\mu_{\uparrow}$ originated from the spin injection across the interface. Even if $\alpha_{\text{NM}} = 0$, $f_{1,s}$ still exists as long as there is a nonzero spin current, for example from $\Delta T = T_2 - T_1 \neq 0$ or $\alpha_{\text{FI}} \neq 0$. Below, we will study j_d , j_m , j_e separately, and by applying the boundary condition given in Eq. (7), and find out the relationship between spin current across the interface, spin accumulation at steady state and ΔT , α_{FI} , α_{NM} . To simplify the presentation, we introduce two notations

$$\begin{aligned} L_1 &= f_0(\mathbf{k})[1 - f_0(\mathbf{k}')]n_0(\mathbf{q}), \\ L_2 &= f_0(\mathbf{k}')[1 - f_0(\mathbf{k})][n_0(\mathbf{q}) + 1]. \end{aligned} \quad (21)$$

Then, $j_d = \hbar C \int_{\text{all}} (L_1 - L_2)$, where $L_1/L_2 = e^{(\beta_1 - \beta_2)\varepsilon_q}$. When $T_2 > T_1$, the magnons have higher temperature, we have $\beta_1 > \beta_2$, $L_1 > L_2$, and $j_d > 0$. The spin current induced by the temperature difference flows from FI to NM. The spin current reverses its direction when $T_1 > T_2$. In general, temperature difference at the interface generates a spin flow from the hotter side to the colder side. When $\Delta T \ll T_1, T_2$, we can expand $L_1/L_2 \approx 1 + (\beta_1 - \beta_2)\varepsilon_q = 1 + \Delta T \frac{\varepsilon_q}{k_{\text{B}} T_1 T_2}$, then $j_d = \mathcal{K}_1 \Delta T$ is proportional to ΔT , and coefficient \mathcal{K}_1 is

$$\mathcal{K}_1 = \hbar C \int_{\text{all}} \frac{\varepsilon_q L_2}{k_{\text{B}} T_1 T_2}. \quad (22)$$

To evaluate j_m , we substitute Eq. (9) into Eq. (19) and, noting that $n_1(-\mathbf{q}) = -n_1(\mathbf{q})$, we obtain

$$j_m = \alpha_{\text{FI}} \hbar C \int_{\text{all}} \left\{ \frac{-\tau v_x(\mathbf{q}) \varepsilon_q}{k_{\text{B}} T_2^2} L_2 \left[(2n_0 + 1) + \Delta T \frac{\varepsilon_q}{k_{\text{B}} T_1 T_2} (n_0 + 1) \right] \right\}. \quad (23)$$

For $\Delta T \ll T_1, T_2$, then $L_1/L_2 \approx 1 + \Delta T \frac{\varepsilon_q}{k_{\text{B}} T_1 T_2}$. For the linear response of the spin current to ΔT , α_{FI} and α_{NM} , we can drop the last term in the bracket in Eq. (23) that would result in a higher order contribution, proportional to $\Delta T \cdot \alpha_{\text{FI}}$. Note that the integration range includes only $q_x < 0$, thus $-v_x(\mathbf{q}) = -\frac{2J}{\hbar} q_x > 0$, $j_m = \mathcal{K}_2 \alpha_{\text{FI}}$ is proportional to α_{FI} , and coefficient \mathcal{K}_2 is

$$\mathcal{K}_2 = \hbar C \int_{\text{all}} \frac{-\tau v_x(\mathbf{q}) \varepsilon_q}{k_{\text{B}} T_2^2} L_2 (2n_0 + 1), \quad (24)$$

which is positive. When $\alpha_{\text{FI}} > 0$ ($T_L < T_R$), the spin current flows from FI to NM, and reverses its direction when $\alpha_{\text{FI}} < 0$. In general, the spin current caused by temperature gradient in FI flows from hotter side to colder side.

In order to compute j_e and because $f_{1,s}$ contains many terms, we decompose j_e into $j_{e,i}$, due to the isotropic part $-\delta\mu_s \frac{\partial f_0(\mathbf{k})}{\partial E}$ of $f_{1,s}$, and $j_{e,a}$, due to the anisotropic part

$g_s(\mathbf{k})$ of $f_{1,s}$,

$$j_{e,i} = \delta\mu_\uparrow(0) \hbar C \int_{\text{all}} \beta_1 L_2 \left\{ \left(\frac{L_1}{L_2} + 1 \right) + \left(\frac{L_1}{L_2} - 1 \right) [f_0(\mathbf{k}') - f_0(\mathbf{k})] \right\} \quad (25)$$

$$j_{e,a} = \hbar C \int_{\text{all}} [a_\uparrow(\mathbf{k})] (-\beta_1 L_2) \left\{ \left(\frac{L_1}{L_2} - 1 \right) [1 - f_0(\mathbf{k})] + [1 - 2f_0(\mathbf{k})] \right\} + [a_\downarrow(\mathbf{k}')] (-\beta_1 L_2) \left\{ [1 - 2f_0(\mathbf{k}')] - f_0(\mathbf{k}') \left(\frac{L_1}{L_2} - 1 \right) \right\}, \quad (26)$$

where

$$a_\uparrow(\mathbf{k}) = \tau_c v_x(\mathbf{k}) \left[\frac{\alpha_{\text{NM}}}{T_1} (E_k - \mu_e) + \frac{d\mu_e}{dx} + \frac{d\delta\mu_\uparrow}{dx} \right],$$

$$a_\downarrow(\mathbf{k}') = \tau_c v_x(\mathbf{k}') \left[\frac{\alpha_{\text{NM}}}{T_1} (E_{k'} - \mu_e) + \frac{d\mu_e}{dx} - \frac{d\delta\mu_\uparrow}{dx} \right]. \quad (27)$$

Since $\delta\mu_\uparrow(0)$ is always small, we keep only linear terms so that all terms with $\left(\frac{L_1}{L_2} - 1\right)$ in Eq. (26,27) are neglected. Then we have $j_{e,i} \approx \mathcal{K}_3 \delta\mu_\uparrow(0)$ and $j_{e,a} \approx \mathcal{K}_4 \alpha_{\text{NM}} + \mathcal{K}_5 \frac{d\mu_e}{dx} + \mathcal{K}_6 \frac{d\delta\mu_\uparrow}{dx}$ with coefficients \mathcal{K}_i ($i = 3, 4, 5, 6$) being

$$\mathcal{K}_3 = \hbar C \int_{\text{all}} \left(\frac{2L_2}{k_B T_1} \right),$$

$$\mathcal{K}_4 = \hbar C \int_{\text{all}} \frac{-\tau_c L_2}{k_B T_1^2} \{ v_x(\mathbf{k}) (E_k - \mu_e) [1 - 2f_0(\mathbf{k})] + v_x(\mathbf{k}') (E_{k'} - \mu_e) [1 - 2f_0(\mathbf{k}')] \},$$

$$\mathcal{K}_5 = \hbar C \int_{\text{all}} \frac{-\tau_c L_2}{k_B T_1} \{ v_x(\mathbf{k}) [1 - 2f_0(\mathbf{k})] + v_x(\mathbf{k}') [1 - 2f_0(\mathbf{k}')] \},$$

$$\mathcal{K}_6 = \hbar C \int_{\text{all}} \frac{-\tau_c L_2}{k_B T_1} \{ v_x(\mathbf{k}) [1 - 2f_0(\mathbf{k})] - v_x(\mathbf{k}') [1 - 2f_0(\mathbf{k}')] \}. \quad (28)$$

Note that \mathcal{K}_4 , \mathcal{K}_5 , \mathcal{K}_6 contain a factor $[1 - 2f_0(\mathbf{k})]$ in the integrals and since only electrons near the Fermi surface participant in scatterings, $[1 - 2f_0(\mathbf{k})] L_2$ is always small. For \mathcal{K}_5 and \mathcal{K}_6 , the factor $(1 - 2f_0) \approx \frac{1}{2} \beta_1 (E - \mu_e)$ which change its sign at the Fermi surface, and the contribution from the electrons above and below the Fermi surface almost cancel each other. For \mathcal{K}_4 , though $(E - \mu_e)(1 - 2f_0) > 0$, but noting that $k_x > 0$ and $k'_x < 0$, the two parts of \mathcal{K}_4 have different sign, and their magnitudes are almost the same. According to the previous section, we have $\frac{d\mu_e}{dx} = -\frac{\alpha_{\text{NM}}}{2T} \frac{(\pi k_B T)^2}{\mu_e}$ and

$\frac{d\delta\mu_\uparrow}{dx} = \frac{\delta\mu_\uparrow}{l_{sd}}$. The non-equilibrium distribution of electrons would induce a spin current as

$$j_e = j_{e,i} + j_{e,a} = \mathcal{K}'_3 \delta\mu_\uparrow(0) + \mathcal{K}'_4 \alpha_{\text{NM}} \quad (29)$$

where $\mathcal{K}'_3 = \mathcal{K}_3 + \frac{1}{l_{sd}} \mathcal{K}_6$ and $\mathcal{K}'_4 = \mathcal{K}_4 - \frac{T(\pi k_B)^2}{2\mu_e} \mathcal{K}_5$. Numerical results in the next section shows that \mathcal{K}'_4 is much smaller than \mathcal{K}_2 and almost zero.

C. Spin current injection and spin accumulation at steady state

Substitute results of $j_{\text{FI} \rightarrow \text{NM}}$ obtained in the previous subsection and Eq. (14) into Eq. (7), we have

$$\mathcal{K}_1 \Delta T + \mathcal{K}_2 \alpha_{\text{FI}} + \mathcal{K}'_4 \alpha_{\text{NM}} + \left(\mathcal{K}'_3 + \frac{\hbar}{2e^2} \frac{\sigma}{l_{sd}} \right) \delta\mu_\uparrow(0) = 0, \quad (30)$$

and, thus spin accumulation at FI/NM interface is

$$\delta\mu_\uparrow(0) = -\frac{2e^2 l_{sd} \mathcal{K}_1}{2e^2 l_{sd} \mathcal{K}'_3 + \hbar \sigma} \Delta T - \frac{2e^2 l_{sd} \mathcal{K}_2}{2e^2 l_{sd} \mathcal{K}'_3 + \hbar \sigma} \alpha_{\text{FI}} - \frac{2e^2 l_{sd} \mathcal{K}'_4}{2e^2 l_{sd} \mathcal{K}'_3 + \hbar \sigma} \alpha_{\text{NM}}. \quad (31)$$

Then the total spin current across the interface is

$$j_{\text{FI} \rightarrow \text{NM}} = \frac{\hbar \sigma \mathcal{K}_1}{\hbar \sigma + 2e^2 l_{sd} \mathcal{K}'_3} \Delta T + \frac{\hbar \sigma \mathcal{K}_2}{\hbar \sigma + 2e^2 l_{sd} \mathcal{K}'_3} \alpha_{\text{FI}} + \frac{\hbar \sigma \mathcal{K}'_4}{\hbar \sigma + 2e^2 l_{sd} \mathcal{K}'_3} \alpha_{\text{NM}}, \quad (32)$$

that flows from hotter side to colder side. $\mathcal{K}_1, \mathcal{K}_2, \mathcal{K}'_3, \mathcal{K}'_4$ are functions of T_1 and T_2 , which can be determined by Eqs. (22), (24) and (28). T_1 and T_2 are determined by model parameters, as shown in Section IV,

$$T_1 = \frac{T_L (R \kappa_{\text{FI}} \kappa_{\text{NM}} + d_{\text{FI}} \kappa_{\text{NM}}) + T_R d_{\text{NM}} \kappa_{\text{FI}}}{R \kappa_{\text{FI}} \kappa_{\text{NM}} + d_{\text{NM}} \kappa_{\text{FI}} + d_{\text{FI}} \kappa_{\text{NM}}},$$

$$T_2 = \frac{T_L d_{\text{FI}} \kappa_{\text{NM}} + T_R (R \kappa_{\text{FI}} \kappa_{\text{NM}} + d_{\text{NM}} \kappa_{\text{FI}})}{R \kappa_{\text{FI}} \kappa_{\text{NM}} + d_{\text{NM}} \kappa_{\text{FI}} + d_{\text{FI}} \kappa_{\text{NM}}}. \quad (33)$$

V. NUMERICAL RESULTS AND DISCUSSION

To have a better idea about the magnitude of the spin current and spin accumulation generated by a thermal gradient, we numerically compute the total spin current $j_{\text{FI} \rightarrow \text{NM}}$ given by Eq. (32) with realistic model parameters of YIG: $S = 23.6$, $J = 1.9 \times 10^{-40}$ J·m², $D = 1.8 \times 10^{-24}$ J, $\tau = 10^{-7}$ s [20, 36], $b_{\text{FI}} = 1.2$ nm; and Pt: $\sigma = 9.4 \times 10^6$ m⁻¹Ω⁻¹, $l_{sd} = 1.5$ nm, $\mu_0 = 9.74$ eV. $\mathcal{J}_{sd} = 1$ meV, $d_{\text{FI}} = 1$ nm, and $d_{\text{NM}} = 15$ nm [11] are used. The temperature difference between two thermal reservoirs is set to $T_R - T_L = 10$ K. In order to know which thermal source is more effective in spin current generation, we first examine the cases when all 10

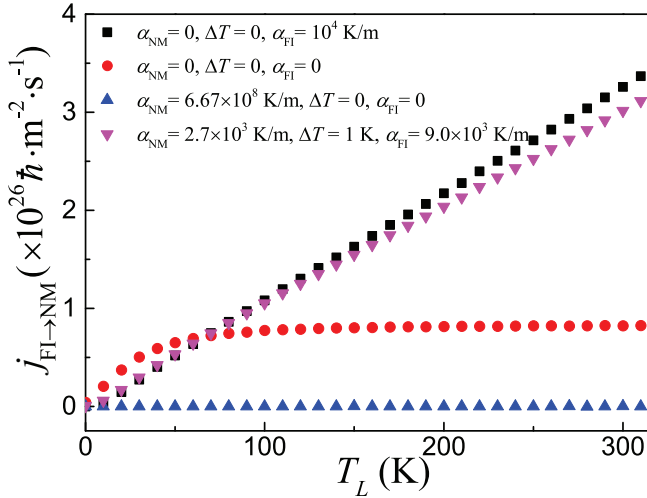


FIG. 2. (color online) Spin current $j_{\text{FI} \rightarrow \text{NM}}$ as a function of T_L when $T_R = T_L + 10$ K for various sets of $\alpha_{\text{NM}}, \alpha_{\text{FI}}$ and ΔT : $\alpha_{\text{NM}} = 0, \alpha_{\text{FI}} = (T_R - T_L)/d_{\text{FI}} = 10^4$ K/m, and $\Delta T = 0$ (black squares); $\alpha_{\text{NM}} = \alpha_{\text{FI}} = 0$, and $\Delta T = 10$ K (red circles); $\alpha_{\text{NM}} = (T_R - T_L)/d_{\text{NM}} = 6.67 \times 10^8$ K/m, $\alpha_{\text{FI}} = 0$, and $\Delta T = 0$ (blue up-triangles); $\alpha_{\text{NM}} = 2.7 \times 10^3$ K/m, $\alpha_{\text{FI}} = 9.0 \times 10^3$ K/m, and $\Delta T = 1$ K (blue up triangles).

K temperature difference is on FI, NM or at the FI/NM interface. The results are shown in Fig. 2 for $\alpha_{\text{NM}} = 0$, $\alpha_{\text{FI}} = (T_R - T_L)/d_{\text{FI}} = 10^4$ K/m, and $\Delta T = 0$ (black squares); $\alpha_{\text{NM}} = \alpha_{\text{FI}} = 0$, and $\Delta T = T_R - T_L = 10$ K (red circles); $\alpha_{\text{NM}} = (T_R - T_L)/d_{\text{NM}} = 6.67 \times 10^8$ K/m, $\alpha_{\text{FI}} = 0$, and $\Delta T = 0$ (blue up-triangles). Although the thermal gradient in NM ($\alpha_{\text{NM}} = 6.67 \times 10^8$ K/m) is four orders of magnitude larger than that in FI ($\alpha_{\text{FI}} = 10^4$ K/m), the spin current due to α_{NM} (up-triangles) is negligibly smaller than that due to α_{FI} (squares), showing ineffective generation of spin current by the thermal gradient in NM. The purple down-triangles in Fig. 2 are $j_{\text{FI} \rightarrow \text{NM}}$ for $\alpha_{\text{NM}} = 2.7 \times 10^3$ K/m, $\Delta T = 1$ K, and $\alpha_{\text{FI}} = 9.0 \times 10^3$ K/m, corresponding to realistic thermal conductivities of $\kappa_{\text{FI}} = 6.0$ W/(m · K) and $\kappa_{\text{NM}} = 20$ W/(m · K) for YIG and Pt [37], and the interfacial thermal resistance of $R = 1.8 \times 10^{-5}$ K/(W/m²). Interestingly, the spin current generated by a thermal gradient in FI increase almost linearly with the temperature while the spin current under a fixed interfacial temperature difference saturates at a higher enough temperature.

The experimentally measured ISHE voltage V in open-circuit comes from ISHE-induced charge accumulation. According to above results, when $T_R > T_L$, spins along the $+z$ -direction move to the $+x$ -direction. Due to the ISHE, a charge current flows along the $+y$ -direction (electrons flow to the $-y$ -direction), resulting in a charge accumulation in the front/back surfaces (xz -planes in Fig. 1) and a higher electric potential in the $+y$ side than that in the $-y$ side as what was observed in experiment [11]. Reversing the direction of either the magnetization of FI or the temperature gradient, the ISHE voltage V changes

sign. The effective electric field along the $+y$ -direction at the interface can be estimated by [31]

$$\frac{1}{d_{\text{NM}}} \int_0^{d_{\text{NM}}} j_s(x) \theta_{\text{SH}} dx = \sigma \mathcal{E}_{\text{avg}}, \quad (34)$$

where θ_{SH} is the spin Hall angle [38] and $V = \mathcal{E}_{\text{avg}} w_{\text{NM}}$, here w_{NM} is the width of the NM layer. Thus, the voltage is given by

$$|V| = \theta_{\text{SH}} \frac{w_{\text{NM}}}{d_{\text{NM}}} \left| \frac{\delta\mu(0)}{e} \right|. \quad (35)$$

For $w_{\text{NM}} = 6$ nm (the same as in the experiment [11]) and for YIG and Pt parameters, the ISHE voltage is estimated to be $60 \mu\text{V}$ that is larger than the experiment value of $6 \mu\text{V}$. The agreement is not too bad since a real system is much more complicated than the ideal model considered here. In reality, the thermal parameters and relaxation times depend on temperature and the structure of a sample. If these complications can be included, our theory may give a more accurate estimate of the ISHE voltage for a sample. In our analysis, we assume the simplest parabolic energy spectrum and constant relaxation times for magnons and electrons. Though the physics shall not change, the value of all quantities should be sensitive to all these parameters. The interface electron-magnon scattering should be important for other phenomena in FI/NM structures such as spin pumping [2, 5–7], transverse SSE [8, 9], spin transfer torque on FI [39] and spin Hall magnetoresistance [40]. It may also be relevant to the concept of “spin mixing conductance”.

VI. CONCLUSION

It is shown that no spin injection and no spin accumulation are possible at the thermal equilibrium. This conclusion is general and model-independent as demanded by the thermodynamical laws. Spin current and spin accumulation can be generated through electron-magnon scatterings by two thermal sources: temperature gradients in FI layers and a temperature difference at NM/FI interface. Both spin current and spin accumulation are sensitive to material properties. The spin accumulation increases and the spin current decreases as the spin diffusion length of NM increases. The spin current arises from imbalance of magnon absorption and emission originated from different magnon and electron temperatures or the deviations of magnons from their equilibrium distributions. Spin current flows from the hotter side to the colder one under a temperature gradient in FI or under an interfacial temperature difference, consistent with existing experiments. In contrast, a temperature gradient in NM cannot efficiently induce a spin current.

VII. ACKNOWLEDGMENT

This work was supported by National Natural Science Foundation of China (Grant No. 11374249). Hong Kong RGC (Grant No. 163011151 and 605413)

-
- [1] I. Žutić, J. Fabian and S. Das Sarma, *Rev. Mod. Phys.* **76**, 323 (2004).
- [2] Y. Kajiwara, K. Harii, S. Takahashi, J. Ohe, K. Uchida, M. Mizuguchi, H. Umezawa, H. Kawai, K. Ando, K. Takanashi, S. Maekawa and E. Saitoh, *Nature (London)* **464**, 262 (2010).
- [3] P. Yan, X. S. Wang, and X. R. Wang, *Phys. Rev. Lett.* **107**, 177207 (2011); D. Hinzke and U. Nowak, *Phys. Rev. Lett.* **107**, 027205 (2011); A. A. Kovalev and Y. Tserkovnyak, *Europhys. Lett.* **97**, 67002 (2012).
- [4] X. S. Wang, P. Yan, Y. H. Shen, G. E. W. Bauer and X. R. Wang, *Phys. Rev. Lett.* **109**, 167209 (2012); B. Hu and X. R. Wang, *Phys. Rev. Lett.* **111**, 027205 (2013).
- [5] C. W. Sandweg, Y. Kajiwara, K. Ando, E. Saitoh, and B. Hillebrands, *Appl. Phys. Lett.* **97**, 252504 (2010).
- [6] B. Heinrich, C. Burrowes, E. Montoya, B. Kardasz, E. Girt, Y.-Y Song, Y. Sun and M. Wu, *Phys. Rev. Lett.* **107**, 066604 (2011).
- [7] M. Weiler, M. Althammer, M. Schreier, J. Lotze, M. Pernpeintner, S. Meyer, H. Huebl, R. Gross, A. Kamra, J. Xiao, Y.-T. Chen, H. Jiao, G. E. W. Bauer and S. T. B. Goennenwein, *Phys. Rev. Lett.* **111**, 176601 (2013).
- [8] K. Uchida, S. Takahashi, K. Harii, J. Ieda, W. Koshibae, K. Ando, S. Maekawa and E. Saitoh, *Nature(London)* **455**, 778 (2008).
- [9] K. Uchida, J. Xiao, H. Adachi, J. Ohe, S. Takahashi, J. Ieda, T. Ota, Y. Kajiwara, H. Umezawa, H. Kawai, G. E. W. Bauer, S. Maekawa and E. Saitoh, *Nat. Mater.* **9**, 894 (2010).
- [10] C. M. Jaworski, J. Yang, S. Mack, D. D. Awschalom, R. C. Mayers and J. P. Heremans, *Phys. Rev. Lett.* **106**, 186601 (2011).
- [11] K. Uchida, M. Ishida, T. Kikkawa, A. Kirihiro, T. Murakami and E. Saitoh, *J. Phys.: Condens. Matter* **26**, 343202 (2014).
- [12] D. Qu, S.Y. Huang, J. Hu, R. Wu and C. L. Chien, *Phys. Rev. Lett.* **110**, 067206 (2013).
- [13] E. Saitoh, M. Ueda, H. Miyajima, and G. Tatara, *Appl. Phys. Lett.* **88**, 182509 (2006).
- [14] G. E. W. Bauer, E. Saitoh, and B. J. van Wees, *Nat. Mater.* **11**, 391399 (2012).
- [15] Y. Tserkovnyak, A. Brataas and G. E.W. Bauer, *Phys. Rev. Lett.* **88**, 117601 (2002).
- [16] J. Xiao, G. E.W. Bauer, K. Uchida, E. Saitoh and S. Maekawa, *Phys. Rev. B* **81**, 214418 (2010).
- [17] S. Hoffman, K. Sato and Y. Tserkovnyak, *Phys. Rev. B* **88**, 064408 (2013).
- [18] H. Adachi, J. Ohe, S. Takahashi and S. Maekawa, *Phys. Rev. B* **83**, 094410 (2011); H. Adachi and S. Maekawa, *J. Korean Phys. Soc.* **62**, 1753 (2013).
- [19] S. A. Bender, R. A. Duine, and Y. Tserkovnyak, *Phys. Rev. Lett.* **108**, 246601 (2012).
- [20] S. S.-L. Zhang and S. Zhang, *Phys. Rev. B* **86**, 214424 (2012).
- [21] J. Ren, *Phys. Rev. B* **88**, 220406(R) (2013).
- [22] S. Y. Huang, W. G. Wang, S. F. Lee, J. Kwo, and C. L. Chien, *Phys. Rev. Lett.* **107**, 216604 (2010); S. Y. Huang, X. Fan, D. Qu, Y. P. Chen, W. G. Wang, J. Wu, T. Y. Chen, J. Q. Xiao, and C. L. Chien, *Phys. Rev. Lett.* **109**, 107204 (2012).
- [23] T. A. Kaplan, *Phys. Rev.* **109**, 782 (1958).
- [24] G. Grosso, G. P. Parravicini, *Solid State Physics*, (Elsevier, Waltham, 2014).
- [25] D. A. Goodings, *Phys. Rev.* **132**, 542 (1963).
- [26] T. Holstein and H. Primakoff, *Phys. Rev.* **58**, 1098 (1940).
- [27] A. Miller and E. Abrahams, *Phys. Rev.* **120**, 745 (1960).
- [28] J. Lu, S. Yin, L. M. Peng, Z. Z. Sun, and X. R. Wang, *Appl. Phys. Lett.* **90**, 052109 (2007).
- [29] E. T. Swartz and R. Q. Pohl, *Rev. Mod. Phys.* **61**, 605 (1989).
- [30] M. Schreier, A. Kamra, M. Weiler, J. Xiao, G. E. W. Bauer, R. Gross, and S. T. B. Goennenwein, *Phys. Rev. B* **88**, 094410 (2013).
- [31] O. Mosendz, V. Vlaminck, J. E. Pearson, F. Y. Fradin, G. E. W. Bauer, S. D. Bader and A. Hoffman, *Phys. Rev. B* **82**, 214403 (2010).
- [32] M. R. Sears and W. M. Saslow, *Phys. Rev. B* **85**, 014404 (2012).
- [33] Shufeng Zhang, *Phys. Rev. Lett.* **85**, 393 (2000)
- [34] T. Valet and A. Fert, *Phys. Rev. B* **48**, 7709 (1993).
- [35] D.K. C. MacDonald, *Thermoelectricity: an Introduction to the Principles*, (Dover Publications, 2006).
- [36] O. Dzyapko, V. E. Demidov, S. O. Demokritov, G. A. Melkov and A. N. Slavin, *New J. Phys.* **9**, 64 (2007).
- [37] Q. G. Zhang, B. Y. Cao, X. Zhang, M. Fujii, K. Takahashi, *J. Phys.: Condens. Matter* **18**, 7937 (2006); A. M. Hofmeister, *Phys. Chem. Miner.* **33**, 45 (2006).
- [38] L. Q. Liu, T. Moriyama, D. C. Ralph, and R. A. Buhrman, *Phys. Rev. Lett.* **106**, 036601 (2011).
- [39] X. Jia, K. Liu, K. Xia and G. E. W. Bauer, *Europhys. Lett.* **96**, 17005 (2011).
- [40] H. Nakayama, M. Althammer, Y.-T. Chen, K. Uchida, Y. Kajiwara, D. Kikuchi, T. Otani, S. Geprägs, M. Opel, S. Takahashi, R. Gross, G. E.W. Bauer, S. T. B. Goennenwein and E. Saitoh, *Phys. Rev. Lett.* **110**, 206601 (2013).